Revista Mexicana de Ingeniería Química

Vol. 12, No. 1 (2013) 121-128

A NEW METHOD TO DETERMINE THE YIELD STRESS OF A FLUID FROM VELOCITY PROFILES IN A CAPILLARY

UN MÉTODO NUEVO PARA DETERMINAR EL ESFUERZO DE CEDENCIA A PARTIR DE LOS PERFILES DE VELOCIDAD EN UN CAPILAR

J.J. López-Durán[1], J. Pérez-González[1*], B.M. Marín-Santibáñez[2] and F. Rodríguez-González[3]

[1]*Laboratorio de Reología, Escuela Superior de Física y Matemáticas, Instituto Politécnico Nacional, U. P. Adolfo López Mateos Edif. 9, Col. San Pedro Zacatenco, C. P. 07738, México D. F., México*
[2]*Sección de Estudios de Posgrado e Investigación, Escuela Superior de Ingeniería Química e Industrias Extractivas, Instituto Politécnico Nacional, U. P. Adolfo López Mateos Edif. 8, Col. San Pedro Zacatenco, C. P. 07738, México D. F., México*
[3]*Departamento de Biotecnología, Centro de Desarrollo de Productos Bióticos, Instituto Politécnico Nacional, Col. San Isidro, C.P. 62731, Yautepec, Morelos, México*

Received 4 of September 2012; Accepted 13 of January 2013

Abstract

A new method to determine the yield stress of a fluid from velocity profiles in capillary flow is presented in this work. The method is based on the calculation of the first derivative of the velocity profiles. For this, the velocity profiles of a model yield stress fluid, 0.2 wt.% Carbopol gel, in a capillary were obtained by using a two dimensional particle image velocimetry system. It is shown that the yield stress value may be reliably determined by using only the velocity profiles and the measured wall shear stresses. This fact is corroborated by independent measurements of the yield stress with a stress controlled vane rheometer. On the other hand, the main details of the flow kinematics of yield-stress fluids were also registered and described in this work. Finally, it was found that the gel slips at the wall with a slip velocity that increases in a power-law way with the shear stress.

Keywords: yield stress, capillary rheometry, particle image velocimetry, Herschel-Bulkley model, wall slip.

Resumen

En este trabajo se presenta un nuevo método para determinar el esfuerzo de cedencia de un fluido a partir de sus perfiles de velocidad en un capilar. El método se basa en el cálculo de la primera derivada de los perfiles de velocidad. Para esto, se obtuvieron los perfiles de velocidad de un fluido modelo con esfuerzo de cedencia, 0.2 wt.% Carbopol gel, en un capilar por medio de velocimetría por imágenes de partículas. Se muestra que el esfuerzo de cedencia se puede determinar de manera confiable usando solamente los perfiles de velocidad y el esfuerzo cortante en la pared. Este hecho es corroborado mediante mediciones independientes del esfuerzo de cedencia con un reómetro de paletas de esfuerzo controlado. Por otro lado, los principales detalles de la cinemática de flujo de fluidos con esfuerzo de cedencia fueron registrados y descritos en este trabajo. Finalmente, se encontró que el gel desliza en la pared del capilar con una velocidad que depende como una ley de potencia del esfuerzo cortante.

Palabras clave: esfuerzo de cedencia, reometría de capilar, velocimetría por imágenes de partículas, modelo de Herschel-Bulkley, deslizamiento.

[*]*Corresponding author. E-mail*: jpg@esfm.ipn.mx
Tel./Fax 55-57-29-60-00, Ext. 55032

1 Introduction

Yield-stress fluids are defined as materials that require the application of a critical shear stress (τ_y) to initiate the flow. Thus, such materials exhibit a solid-like behavior for shear stresses below τ_y and then flow for shear stresses above τ_y. In practice, a large amount of daily use products display this also called viscoplastic behavior, including foods, cleaning products, emulsions, pastes and concrete among many others.

The existence of a yield stress has been a matter of debate for a long time, since its measured value depends on the experimental conditions, as sample preparation, as well as on the sensitivity of the rheometer utilized (Barnes and Walters, 1985; Nguyen and Boger, 1992; Barnes, 1999; Watson, 2004). From the practical point of view, however, the concept of yield stress has been widespread and has become very helpful in industry. For example, the yield stress is a useful parameter for the assessment of shelf-life of paints and other consuming products.

The steady shear properties of yield-stress fluids have been measured mainly by using torsional rheometers. Provided that slip is restricted, a stress controlled rotational rheometer can give a relatively fast and meaningful value of the yield stress (Keentok, 1982). On the contrary, pressure-driven rheometers, as the capillary one, do not have the acceptation of their torsional counterparts for yield-stress fluids characterization. The main reason for this is that experiments with capillaries are very time consuming and the results may be affected by slip at the capillary wall. In spite of this, capillary flow is present in many practical applications where the flow takes place at high shear rates, hence, a direct method to determine the conditions to initiate the flow, i.e., the yield stress, in this type of flow would be desirable.

Magnin and Piau (1990) have stated that it is not possible to carry out rheometrical tests with yield-stress fluids without knowing the real kinematic field. However, as it happens with other rheological systems, most of the analysis of the flow of yield-stress fluids has been mainly done by rheometrical (mechanical) measurements, and the study of their kinematics in different geometries has received limited attention. Therefore, in the present work, a detailed analysis of the flow of a model yield-stress fluid, 0.2 wt.% Carbopol gel, in a capillary has been carried out by using particle image velocimetry (PIV) along with rheometrical measurements, which, to our knowledge, has not been made. PIV is a powerful non-invasive technique used to describe the flow kinematics in transparent fluids. Also, PIV is a whole-field method that allows for the determination of instantaneous velocity maps in a flow region. This last approach, of common use in fluid mechanics, has been gradually implemented for the analysis of the flow behavior of complex fluids (Pérez-González *et al*., 2012). Thus, by using PIV, we have been able to capture the main details of the flow development of a yield-stress fluid in the presence of slip at the wall. The results in this work show that the behavior of the fluid agrees well with the existence of a yield stress, which can be reliably determined from the velocity profiles and the measured wall shear stress.

2 Theory

Yield-stress fluids have been studied by theoretical and experimental methods and the main results are summarized in a series of reviews by different authors (see for example Cheng, 1986; Nguyen and Boger, 1992; Denn and Bonn, 2011). The simplest yield-stress fluid, also known as the Bingham fluid, is described by the constitutive equation:

$$\tau = \tau_y + \eta_p \dot{\gamma}, \tau > \tau_y \quad \& \quad \dot{\gamma} = 0, \tau \leq \tau_y \qquad (1)$$

where τ is the shear stress, τ_y is the yield stress; η_p is known as the plastic viscosity and $\dot{\gamma}$ is the shear rate. Eq. (1) predicts a Newtonian behavior once the fluid starts flowing. In practice, however, most fluids with a yield stress are shear-thinning. Thus, generalizations to account for the effect of shear-thinning have been introduced. A widespread model is the Hershel-Bulkley's one, given by:

$$\tau = \tau_y + k\dot{\gamma}^n, \tau > \tau_y, \quad \& \quad \dot{\gamma} = 0, \tau \leqslant \tau_y \qquad (2)$$

Where k and n have the typical meaning of consistency and shear-thinning index, respectively.

The characteristic flow curve of a yield-stress fluid contains a region of true flow preceded by another region without flow, but in which, slip may be present (Fig. 1). The transition between such regions, *i. e.*, the yielding behavior, depends on whether slip is present or not (see for example Fig. 4 in Nguyen and Boger, 1992). In the presence of slip in a capillary rheometer of given length (L) to diameter (D) ratio (L/D), the flow curve depends on the capillary diameter as well, and the transition between both regions is expected to be sharper for bigger diameters in shear-thinning fluids.

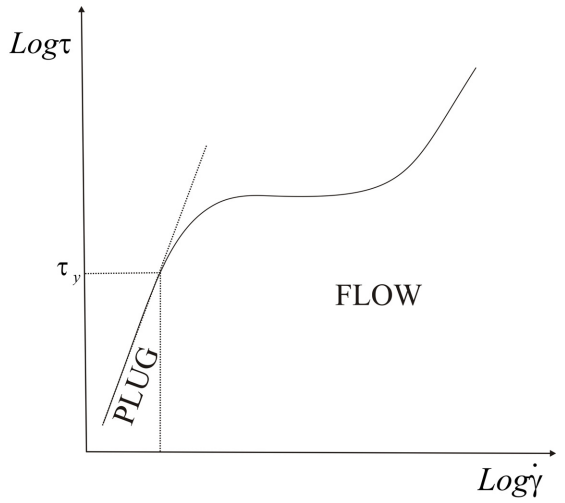

Fig. 1. Schematic flow curve of a yield stress fluid. The vertical dashed line limits the solid-like behavior of the fluid, while the horizontal dotted line indicates the yield stress value.

Thus, the yield stress may be determined by finding the critical shear stress at the transition between the two regions. The accuracy on the determination of such a value will depend on the sharpness of the transition as well as on the density of experimental points. Nevertheless, the yield stress, being a property of the material, should be independent of the capillary diameter.

It is important to notice at this point that a single flow curve does not provide indication for the existence of a yield stress nor for the presence of slip. Moreover, the flow curve alone does not give information on the characteristics of the different flow regimes and additional information is required for a full description of the flow behavior of the fluid. Rodríguez-González *et al*. (2009) have shown that the calculation of the slip velocity and the whole analysis of the kinematics in capillary flow may be carried out, without using different capillary diameters, by means of the PIV technique. Thus, the velocity profiles may be used to calculate the yield stress of the fluid as shown below.

The construction of the flow curves for capillary flow is based on the wall shear stress (τ_w) and the apparent shear rate ($\dot{\gamma}_{app}$) which are calculated as (Bird *et al*., 1977):

$$\tau_w = \frac{\Delta p}{\left(4\frac{L}{D}\right)} \tag{3}$$

$$\dot{\gamma}_{app} = \frac{32Q}{\pi D^3} \tag{4}$$

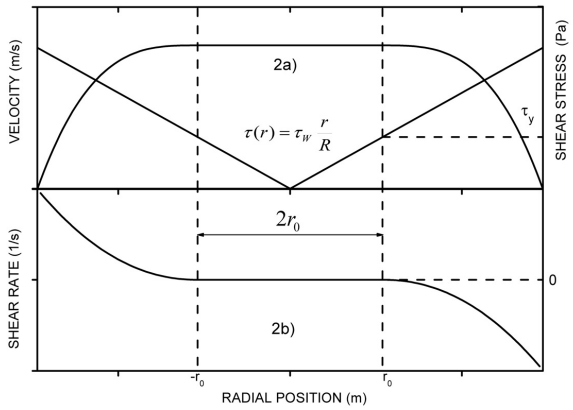

Fig. 2. a) Schematic velocity profile of a Herschel-Bulkley fluid and the shear stress profile in a capillary. b) Derivative of the Herschel-Bulkley velocity profile with respect to the radial position. Vertical dashed lines indicate the yielding position (r_0) in the velocity and shear rate profiles, respectively.

where Δp is the pressure drop between capillary ends and Q is the volumetric flow rate. Figure 2a shows a schematic velocity profile $v_z(r)$ of a yield-stress shear-thinning fluid in a capillary described the Herschel-Bulkley model (Coussot, 2005):

$$v_z(r) = \left(\frac{\tau_w}{k}\right)^{1/n} \frac{nR}{n+1}\left(1 - \frac{r_0}{R}\right)^{(n+1)/n}; 0 \le r \le r_0 \tag{5}$$

$$v_z(r) = \left(\frac{\tau_w}{k}\right)^{1/n} \frac{nR}{n+1}\left[\left(1 - \frac{r_0}{R}\right)^{(n+1)/n} - \left(\frac{r}{R} - \frac{r_0}{R}\right)^{(n+1)/n}\right]; \quad r_0 < r \le R \tag{6}$$

where k and n have the typical meaning of consistency and shear-thinning index, respectively; r_0 is the critical radial position at which the yield stress is reached and R is the capillary radius. Since the shear stress (τ) tends to zero as r approaches to the capillary axis ($\tau(r) = r\tau_w/R$), there will always be an unsheared (plug) region around the center, whose size decreases with increasing the wall shear stress beyond τ_y, namely, $r_0 = \tau_y R/\tau_w$. This means that more fluid in the capillary yields as τ_w is increased, meanwhile the yielded region approaches asymptotically to the capillary center.

Then, the yield stress may be calculated directly from the velocity profiles via their first derivative. According to the shape of a velocity profile, its first derivative, which also represents the true shear rate for a unidirectional flow, must become zero at the position where the shear stress reaches the yield value. Fig. 2b shows the first derivative of the velocity as a function

of the radial position (dv/dr) for the profile sketched in Fig. 2a. The position at which $dv/dr = 0$ in Fig. 2b is found as r_0 and then, $\tau_y = r_0\tau_w/R$.

The numerical derivative of the velocity profiles with respect to the radial position may be calculated by a central difference approximation as shown below:

$$\left(\frac{\partial v_z}{\partial r}\right)_i = \frac{1}{2}\left(\frac{v_{i+1} - v_i}{r_{i+i} - r_i} + \frac{v_i - v_{i-1}}{r_i - r_{i-1}}\right) \qquad (7)$$

where v_i indicates the local axial velocity at the ith radial position, r_i, respectively ($i = 1, \ldots, N$, where N indicates the total points in the experimental velocity profile).

3 Materials and methods

The system studied here was a physical gel of Carbopol at a temperature of 25 °C. Carbopol is a polyacrylic acid that produces an acid solution when dispersed in water. Neutralization of the solution with a base results in a gel with plasticity and viscoelastic behavior (Piau, 2007). Neutralized gels made up of Carbopol are inexpensive, transparent and harmless materials with many applications, being the gel for hair one of the most popular. In addition, Carbopol gels have been used as model systems for the study of the flow behavior of viscoplastic materials.

In order to make the gel, a solution was first prepared by dissolving 0.2 wt.% of Carbopol 940 (BF Goodrich) in tri-distilled water. Then, hollow glass spheres (as tracers for PIV) of 12 μm of average diameter (Sphericel 110 P8, Potters Industries), in a concentration of 0.2 wt.% were dispersed in the solution, which was further neutralized, according to the Carbopol content, with sodium hydroxide.

Rheological measurements were performed in a pressure controlled capillary rheometer with a borosilicate glass capillary of L = 0.298 m and D =0.00294 m (L/D = 101.4). This large L/D ratio makes unnecessary pressure corrections for end effects. The reservoir from which the fluid was fed as well as the capillary were kept in a controlled temperature water bath at 25.0 ± 0.2 °C, but one part of the capillary remained out of the bath for PIV measurements. The pressure drop between capillary ends was measured with a Validyne® differential pressure transducer and the flow rate was determined by collecting and measuring the ejected mass as a function of time. Only variations of around 1% in the flow rate were allowed for a given pressure condition to consider the flow as steady.

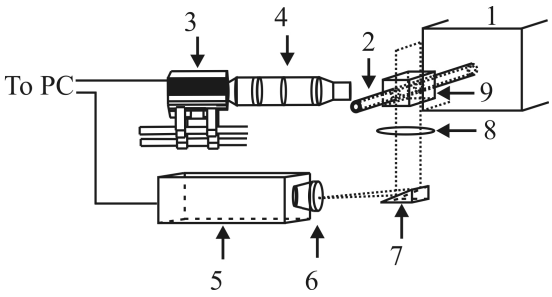

Fig. 3. Experimental set up. 1) Water bath, 2) glass capillary, 3) CCD camera, 4) microscope, 5) Nd:YAG Laser, 6) Cylindrical lens, 7) prism, 8) biconvex lens, 9) aberration corrector.

On the other hand, a stress controlled Paar Physica UDS 200 rotational rheometer with the FL 100 vane geometry was also utilized as an independent way to measure the yield stress.

The study of the flow kinematics in the capillary was performed with a two dimensional PIV Dantec Dynamics system as sketched in Fig. 3. This system has been previously used for the analysis of the flow kinematics of micellar solutions (Marín-Santibañez *et al*., 2006) and polymer melts (Rodriguez-Gonzalez *et al*., 2009, 2010, 2011) in capillaries. All the details of the PIV set up to analyze capillary flow may be found elsewhere and only a brief description is presented here.

The PIV system consists of a high speed and high sensitivity HiSense MKII CCD camera of 1.35 Mega-pixels, two coupled Nd:YAG lasers of 50 mJ with λ = 532 nm and the Dantec Dynamic Studio 2.1 software. A light sheet was reduced in thickness up to less than 200 μm by using a biconvex lens with 0.05 m of focal distance, and sent through the center plane of the capillary. An InfiniVar® continuously-focusable video microscope CFM-2/S was attached to the CCD camera in order to increase the spatial resolution.

The images taken by the PIV system covered an area of 0.00294 m × 0.00231 m which was located around an axial position of z = 75D downstream from the contraction. Series of fifty image pairs were obtained for each flow condition once the steady state was reached, and all the image pairs were correlated to obtain the corresponding velocity map. Then, the fifty velocity maps were averaged in time to obtain a single one, from which, the velocity as a function of the radial position (velocity profile) was obtained for the desired axial position.

4 Results and discussion

4.1 Capillary rheometry

Figure 4 shows the capillary flow curve for the gel (filled symbols), along with the one obtained from the integration of the velocity profiles (hollow symbols) according to:

$$Q = \int_0^{2\pi} \int_0^{R} r v_z(r) dr d\theta \qquad (8)$$

Validation of the PIV measurements is performed by their direct comparison with rheometrical data in the flow curve. In this case, the data obtained from the velocity profiles agree well with the rheometrical ones; the maximum difference in the volumetric flow rates obtained by using the two methods was 6.5%, which shows the reliability of the PIV technique to describe the behavior of the gel in capillary flow.

The flow curve covers a volumetric flow rate range from 10^{-8} to 10^{-6} m^3/s (corresponding to an apparent shear rate range of about 300 s^{-1}), and has been divided into two regions (I and II). Region I appears linear in the log-log plot and has, therefore, been fitted by a power-law equation (see the equations inserted in Fig. 4). The other region (II) contains a fairly smooth transition linked to straight line.

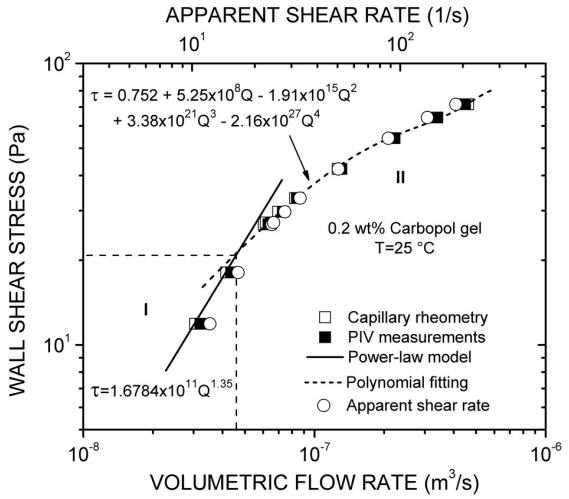

Fig. 4. Wall shear stress vs. volumetric flow rate for the Carbopol gel. Open and filled symbols correspond to rheometrical and PIV measurements, respectively. The flow curve was divided into two regions: (I) solid-like behavior (pure slip) and (II) flow with slip. The continuous and dashed lines represent the fitting to models.

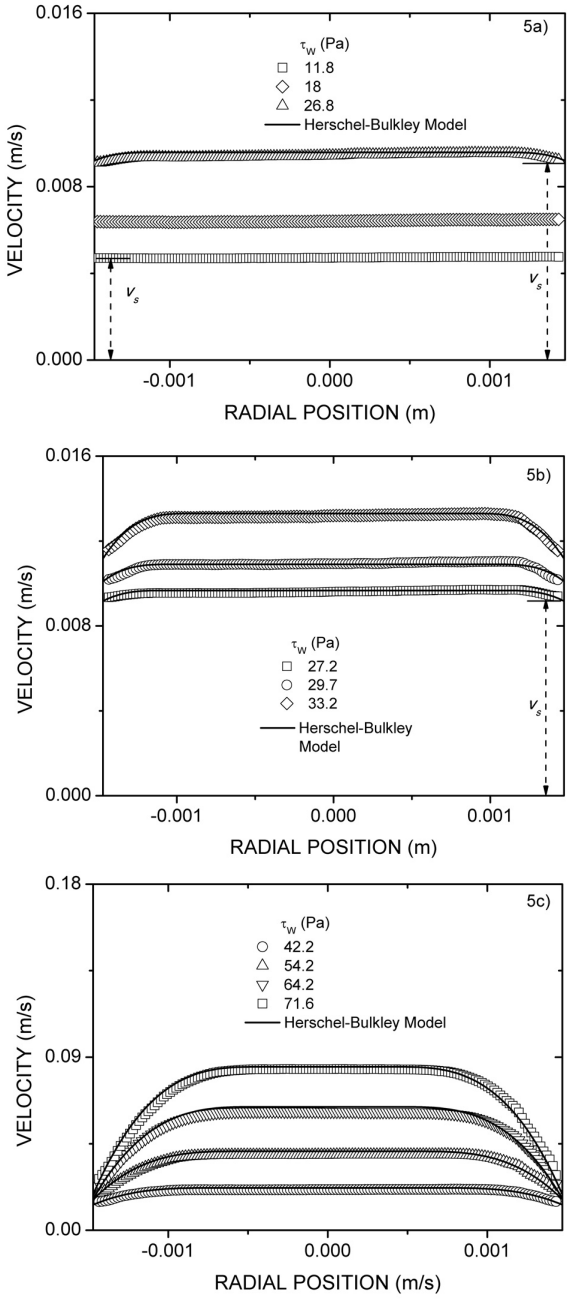

Fig. 5. Velocity profiles for different wall shear stresses for the Carbopol gel. a) 11.8 Pa, 18 Pa and 26.8 Pa; b) 27.2 Pa, 29.7 Pa and 33.2 Pa; c) 42.2 Pa, 54.2 Pa, 64.2 Pa and 71.6 Pa.

The volumetric flow rate limiting regions I and II was established as that at the intersection of the straight line in region I with the curve in region II.

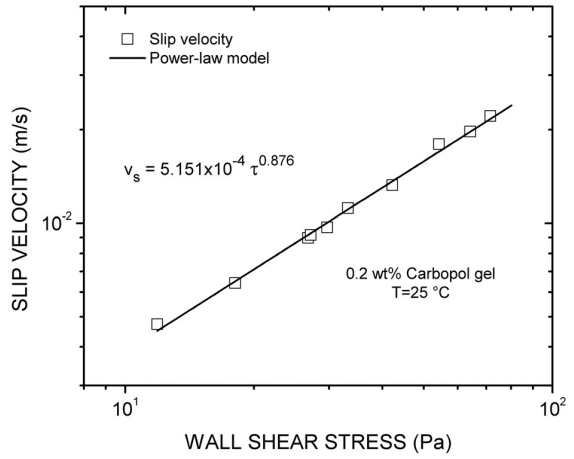

Fig. 6. Slip velocity vs. wall shear stress for the Carbopol gel. The continuous line represents the fitting to a power-law model.

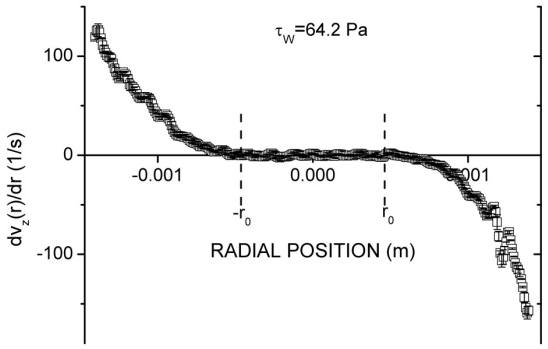

Fig. 7. First derivative of the velocity as a function of the radial position for the profile obtained at τ_w = 64.2 Pa. Vertical dashed lines indicate the position at which $dv/dr = 0$ ($r_0 = 0.000463 \pm 0.000032$ m), which corresponds to $\tau_y = 20.2 \pm 1.4$ Pa.

4.2 *Description of the flow kinematics*

Figures 5a-c show the velocity profiles for the different flow conditions investigated in this work, which clearly exhibit the changes in the velocity field with increasing the wall shear stress, namely, the profiles change from completely plug-like to shear-thinning like with a non-yielded region and slip at the wall. The average of the standard deviations for each profile was around 1%, which is of the size of the symbols used to represent the data. On the other hand, an analysis of the velocity maps (they are not shown here for the sake of space) shows that the velocity in the radial direction was at least three orders of magnitude smaller than the axial one in each case. Thus, the velocity profiles in Figs. 5a-c represent a unidirectional flow and the velocity field is simply given by $v_z = v_z(r)$ for the different shear stresses, as it is expected for a fully developed shear flow.

Figure 5a shows that for shear stresses in region I (below the yield value), the velocity profiles appear completely flat or plug-like, which is characteristic of a solid-like behavior. Then, region I in the flow curve may be attributed to plug flow. Under these conditions, the flow rate is only due to slip of the gel at the capillary wall. At the shear stress of 26.8 Pa, it is possible to appreciate a slight development of flow near the capillary wall (see the highest profile in Fig. 5a), even though the velocity profile appears almost flat. Thus, this shear stress value, which is the first experimental point taken in region II, cannot be considered as corresponding to the yield stress, since it already includes a flow development. Consequently, an accurate determination of the yield stress by using the pure rheometrical data require of a large number of experimental points, which would be very impractical. One way to face this problem is discussed in the next section.

Beyond the yield stress, the velocity profiles in Figs. 5b-c show the plug-like region around the capillary axis and shear-thinning, both characteristic of a yield-stress fluid. In addition, the velocity profiles clearly exhibit a non-zero velocity at the wall, i. e., the gel slips at the capillary wall with a velocity (v_s) that increases along with the wall shear stress (Fig. 6).

4.3 *Determination of the yield stress from velocity profiles*

As discussed in the previous section, an accurate determination of the yield stress by using the pure rheometrical data would require of a large number of experimental points, which would be impractical. This problem can be overcome by calculating the yield stress directly from the velocity profiles via their first derivative. For this, the true shear rate must be zero at the position where the shear stress reaches the yield value. Meanwhile, the corresponding shear stress is given by $\tau(r) = r\tau_w/R$. Figure 7 shows the first derivative of the velocity as a function of the radial position (dv/dr) for the profile obtained at τ_w = 64.2 Pa. The position at which $dv/dr = 0$ in Fig. 7 is found as $r_0 = 0.000463 \pm 0.000032$ m, which corresponds to a shear stress value of 20.2 ± 1.4 Pa. If the same analysis is performed with all the velocity profiles in

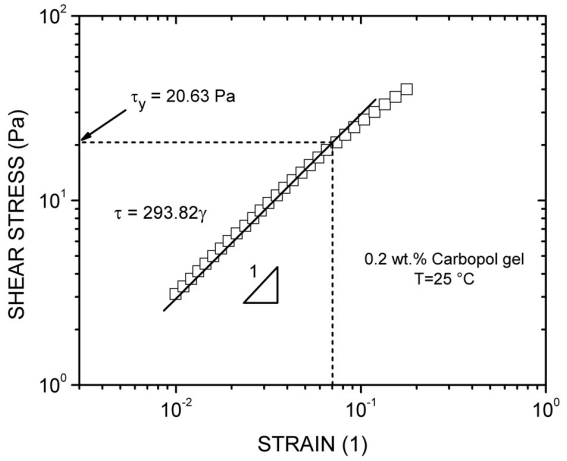

Fig. 8. Shear stress vs. shear strain for the Carbopol gel. The continuous line represents the fitting to the Hooke model.

figs. 5b-c, considering the symmetry of the profiles (i. e., the values obtained at both sides of the profiles), an average value of 20.5 ± 1.2 Pa is obtained.

Once the yielding position and the yield stress are determined, they can be inserted in Eqs. (5) and (6) to calculate the velocity profiles. Note that the experimental velocity profiles in Figs. 5a-c are very well described by the Herschel-Bulkley model (Eqs. 5-6) with k = 3.679 Pa s$^{0.5}$ and n = 0.5, which gives further support to the reliability of the yield stress calculated from the velocity profiles.

4.4 Determination of the yield stress from vane rheometry

Figure 8 shows the results of an analysis of the gel by a slow shear stress ramp in the vane rheometer. In this case, we have made use of the fact that for a solid-like behavior the relationship between the shear stress and shear deformation (γ) should be linear (Hookean behavior). It may be observed that the torque changes linearly with γ up to a value of 0.07, and then deviates from the linearity. The first experimental point considered as lying out of the straight line had a deviation of 6.3% in the torque value. The previous experimental point, which had a deviation of only 4.75% with respect to the solid-like behavior, was used to calculate the yield stress for the gel as 20.6 ± 0.9 Pa, which is in very good agreement with the yield stress value obtained from the velocity profiles.

Summarizing, the yield stress values obtained from the different analysis are in good agreement, which shows that the new method presented here, based on the first derivative of the velocity profiles, is reliable and may be used for other fluids, provided that the velocity profiles are available.

Conclusions

The yielding and flow behavior of a model yield-stress fluid, 0.2 wt.% Carbopol gel, in a capillary with slip at the wall was investigated in this work by PIV. The flow behavior consists in a purely plug-like flow before yielding, followed by shear thinning with slip at relatively high shear rates. The velocity profiles were well described by the Herschel-Bulkley model and allowed for a reliably determination of the yield stress. The method presented here may be used for other fluids, provided that the velocity profiles are available. Finally, the slip velocity was found to increase in a power-law way with the shear stress.

Acknowledgements

This research was supported by SIP-IPN (No. Reg. 20131369). J J. L.-D. had a PFI-IPN scholarship to perform this work and J. P.-G, B. M. M.-S and F. R-G are COFAA-EDI fellows.

Nomenclature

L	length of the capillary
D	diameter of the capillary
R	radius of the capillary
r	radial position
r_0	radial position at which the yield stress is reached
z	axial position
v_z	axial velocity
Δp	pressure drop
Q	volumetric flow rate
k	consistency index
n	shear-thinning index
Greek symbols	
τ	shear stress
τ_w	wall shear stress
τ_y	yield stress
γ	shear strain
$\dot{\gamma}$	shear rate
$\dot{\gamma}_{app}$	apparent shear rate
$\dot{\gamma}_r$	shear rate at a certain radial position
$\dot{\gamma}_R$	shear rate at $r = R$
η	shear viscosity
η_p	plastic viscosity

References

Barnes H.A. (1999). The yield stress-a review or '$\pi\alpha\nu\tau\alpha\rho\epsilon\iota$'-everything flows? *Journal of Non-Newtonian Fluid Mechanics 81*, 133-178.

Barnes H.A., Walters K. (1985). The yield stress myth? *Rheologica Acta 24*, 323-326.

Bird R.B., Armstrong R.C., Hassager O. (1977). *Dynamics of polymeric liquids*. Vol. 1. John Wiley & Sons. USA.

Cheng D. C.-H. (1986). Yield stress: A time-dependent property and how to measure it. *Rheologica Acta 25*, 542-554.

Coussot P. (2005). *Rheometry of pastes, suspensions, and granular materials*. Wiley-Interscience, USA.

Denn M.M., Bonn D. (2011). Issues in the flow of yield-stress liquids. *Rheologica Acta 50*, 307-315.

Keentok M. (1982). The measurements of the yield stress of liquids. *Rheologica Acta 21*, 325-332

Magnin A., Piau J.M. (1990). Cone-and-plate rheometry of yield stress fluids. Study of an aqueous gel. *Journal of Non-Newtonian Fluid Mechanics 36*, 85-108.

Marín-Santibañez B.M., Pérez-González J., de Vargas L., Rodríguez-González F., Huelsz G. (2006). Rheometry-PIV of shear thickening wormlike micelles. *Langmuir 22*, 4015-4026.

Nguyen Q.D., Boger D.V. (1992). Measuring the flow properties of yield stress fluids. *Annual Review of Fluid Mechanics 24*, 47-88.

Piau J.M. (2007). Carbopol gels: elastoviscoplastic and slippery glasses made of individual swollen sponges meso-and macroscopic properties, constitutive equation and scaling laws. *Journal of Non-Newtonian Fluid Mechanics 144*, 1-29.

Pérez-González J., Marín-Santibáñez B.M., Rodríguez-González F., González-Santos G. (2012). Rheo-Particle Image Velocimetry for the Analysis of the Flow of Polymer Melts. In: *Particle Image Velocimetry* (Cavazzini G, ed.), Pp 203-228, Intech, Croatia.

Rodríguez-González F., Pérez-González J., de Vargas L., Marín-Santibáñez B.M. (2010). Rheo-PIV analysis of the slip flow of a metallocene linear low-density polyethylene melt. *Rheologica Acta 49*, 145-154.

Rodríguez-González F., Pérez-González J., Marín-Santibáñez B.M. (2011). Analysis of capillary extrusion of a LDPE by PIV. *Revista Mexicana de Ingeniería Química 10*, 401-408.

Rodríguez-González F., Pérez-González J., Marín-Santibáñez B.M., de Vargas L. (2009). Kinematics of the stick-slip capillary flow of high-density polyethylene. *Chemical Engineering Science 64*, 4675-4683.

Watson J.H. (2004). The diabolical case of the recurring yield stress. *Applied Rheology 14*, 40-45.